Interleaved Cuk Converter Wave Energy System With Advanced Control and Grid Support Functions for Seamless Integration

Preprint

Vikram Roy Chowdhury and Kumaraguru Prabakar

National Renewable Energy Laboratory

Presented at the 50th Annual Conference of the IEEE Industrial Electronics Society (IECON)
Chicago, Illinois
November 3–6, 2024

NREL is a national laboratory of the U.S. Department of Energy
Office of Energy Efficiency & Renewable Energy
Operated by the Alliance for Sustainable Energy, LLC

This report is available at no cost from the National Renewable Energy Laboratory (NREL) at www.nrel.gov/publications.

Contract No. DE-AC36-08GO28308

Conference Paper
NREL/CP-5D00-90095
December 2024

Interleaved Cuk Converter Wave Energy System With Advanced Control and Grid Support Functions for Seamless Integration

Preprint

Vikram Roy Chowdhury and Kumaraguru Prabakar

National Renewable Energy Laboratory

Suggested Citation
Chowdhury, Vikram Roy, and Kumaraguru Prabakar. 2024. *Interleaved Cuk Converter Wave Energy System With Advanced Control and Grid Support Functions for Seamless Integration: Preprint*. Golden, CO: National Renewable Energy Laboratory. NREL/CP-5D00-90095. https://www.nrel.gov/docs/fy25osti/90095.pdf.

NREL is a national laboratory of the U.S. Department of Energy
Office of Energy Efficiency & Renewable Energy
Operated by the Alliance for Sustainable Energy, LLC

This report is available at no cost from the National Renewable Energy Laboratory (NREL) at www.nrel.gov/publications.

Contract No. DE-AC36-08GO28308

Conference Paper
NREL/CP-5D00-90095
December 2024

National Renewable Energy Laboratory
15013 Denver West Parkway
Golden, CO 80401
303-275-3000 • www.nrel.gov

NOTICE

This work was authored in part by the National Renewable Energy Laboratory, operated by Alliance for Sustainable Energy, LLC, for the U.S. Department of Energy (DOE) under Contract No. DE-AC36-08GO28308. Funding provided by the U.S. Department of Energy Office of Energy Efficiency and Renewable Energy Water Power Technologies Office. The views expressed herein do not necessarily represent the views of the DOE or the U.S. Government.

Cover Photos by Dennis Schroeder: (clockwise, left to right) NREL 51934, NREL 45897, NREL 42160, NREL 45891, NREL 48097, NREL 46526.

Interleaved Cuk Converter Wave Energy System With Advanced Control and Grid Support Functions for Seamless Integration

Vikram Roy Chowdhury, Kumaraguru Prabakar and Ben McGilton

National Renewable Energy Laboratory
Denver, CO 80401 USA

***Abstract*—This paper presents an innovative wave energy conversion system that integrates an interleaved Cuk converter with advanced nonlinear control for seamless grid integration. The system efficiently extracts power on the DC side using the interleaved Cuk converter, while an inverter manages power transfer to the grid or load on the AC side. A nonlinear control architecture, based on the Lyapunov energy function, ensures stable and optimal operation under varying wave conditions, effectively addressing the challenges of variability and unpredictability inherent in wave energy. The proposed system also incorporates features to enhance power quality and minimize losses, making it a robust solution for renewable energy integration. The system's effectiveness in harnessing wave energy and achieving smooth grid integration is validated through comprehensive computer simulations in $MATLAB/Simulink$, with case study results demonstrating its capabilities.**

***Index Terms*—interleaved Cuk converter (ICC), wave energy converters ($WECs$), three-phase grid-connected system, Lyapunov energy function, point of common coupling (PCC), pulse width modulation (PWM)**

I. Introduction

THE growing demand for clean and renewable energy has led to a surge in interest in oceanic resources, particularly wave energy [1]–[3]. Wave energy holds immense, largely untapped potential as a reliable and sustainable power source, offering significant environmental and economic advantages. To harness this energy effectively, the development of innovative wave energy conversion systems is essential [4], [5]. Recent research has focused on creating advanced wave energy converters ($WECs$) that can efficiently capture energy from ocean waves and integrate it with existing power grids. Among the various WEC designs, the interleaved Cuk converter (ICC)-based system emerges as a promising solution due to its high efficiency, compactness, and suitability for grid integration. Additionally, incorporating advanced nonlinear control strategies enhances system stability and performance under varying wave conditions, ensuring continuous and reliable energy output. This paper introduces an integrated wave energy conversion system that combines ICC technology with sophisticated nonlinear control for seamless grid integration, even under fluctuating wave environments. Building on prior research, this study demonstrates the proposed system's effectiveness through detailed case studies and performance evaluations, providing evidence of its potential for widespread application. By advancing wave energy conversion technology, this research significantly contributes to the ongoing pursuit of sustainable energy generation and environmental protection. The innovative approaches developed in this study not only improve the efficiency and viability of wave energy systems but also address critical challenges such as system resilience, cost-effectiveness, and long-term sustainability. Furthermore, the research aligns with global efforts to mitigate climate change, reduce carbon emissions, and safeguard marine ecosystems, highlighting the essential role of technological innovation in achieving a sustainable future. The findings and innovations presented here support the global transition to cleaner energy while aligning with initiatives to reduce carbon emissions and protect marine ecosystems. This research plays a vital role in promoting a greener future and driving the technological advancements necessary for sustainable development.

This paper introduces a novel solution to address the challenges associated with wave energy conversion by developing an integrated system based on ICC technology. Current wave energy converters ($WECs$) often struggle with inefficient power extraction and lack robust control strategies necessary for stable grid integration [6]–[8]. This gap underscores the urgent need for advanced wave energy conversion systems that can effectively capture wave energy while ensuring seamless and reliable grid integration. In response to this need, the proposed research focuses on developing an integrated wave energy conversion system utilizing ICC technology. The primary objective is to design and implement advanced nonlinear control techniques that optimize the performance of the ICC in extracting wave energy. By enhancing both the efficiency and stability of the system, this work aims to promote the widespread adoption of wave energy as a viable renewable energy source, thereby supporting the transition to a sustainable energy future. On the AC side, the system integrates with the grid through two-level, three-phase inverters, which operate under an advanced nonlinear control architecture grounded in the Lyapunov energy function, similar

This work was authored by the National Renewable Energy Laboratory, operated by Alliance for Sustainable Energy, LLC, for the U.S. Department of Energy (DOE) under Contract No. DE-AC36-08GO28308. Funding provided by U.S. Department of Energy Office of Energy Efficiency and Renewable Energy Water Power Technologies Office. The views expressed in the article do not necessarily represent the views of the DOE or the U.S. Government. The U.S. Government retains and the publisher, by accepting the article for publication, acknowledges that the U.S. Government retains a nonexclusive, paid-up, irrevocable, worldwide license to publish or reproduce the published form of this work, or allow others to do so, for U.S. Government purposes.

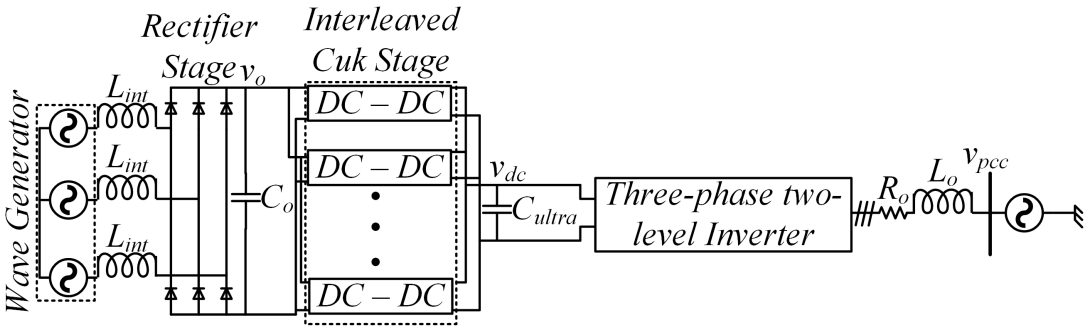

Fig. 1. Simplified diagram of the proposed $WECs$

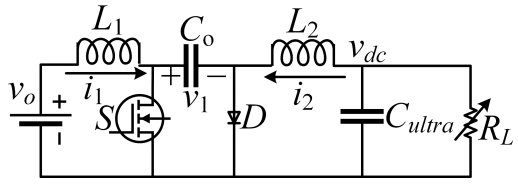

Fig. 2. Simplified circuit diagram for single Cuk converter for the $DC-DC$ stage

to approaches found in [9]–[11]. This control strategy not only ensures smooth power transfer but also adapts dynamically to changing wave conditions, maximizing energy output. Additionally, the proposed system incorporates advanced grid support functions based on IEEE Std 1547 to further enhance grid stability and power quality [12]. These features make the system highly resilient, capable of maintaining performance even in adverse grid conditions. To validate the effectiveness of the proposed approach, the entire system is modeled in $MATLAB/Simulink$, and various critical corner case studies are conducted. The structure of the paper is as follows: Section II details the architecture of the interleaved Cuk converter and its control mechanisms, Section III discusses the Lyapunov energy function-based control for the AC side along with the implemented advanced grid support functions, Section IV presents the results and discussions of the various case studies, and the conclusion is provided in Section V.

II. Interleaved Cuk Converter Modeling and Control

The simplified diagram for the proposed WEC is presented in Fig. 1. The left side is connected to the wave generator stage, which is connected through an interfacing inductor, L_{int}, to a rectifier stage. The output of the rectifier is connected through a capacitor, C_o, to the ICC-based $DC-DC$ stage. Finally, it is connected through an ultra-capacitor (C_{ultra})-based DC bus to a three-phase, two-level inverter connected through an RL filter with parameters R_o and L_o to the point of common coupling (PCC). This section presents the state-space modeling for the Cuk converter to implement the Lyapunov energy function-based controller. A simplified circuit diagram for a single Cuk converter for the ICC, $DC-DC$ stage is presented in Fig. 2. where L_1 and L_2 are the inductors of the Cuk converter, with their corresponding currents as i_1 and i_2, respectively. The input of the Cuk converter is the output of the rectifier i.e., v_o. The output of the Cuk converter is connected to the input of the two-level inverter, i.e., C_{ultra}. To design a Lyapunov energy function-based control architecture, the state-space model of the system is considered in modes 1 (S is on) and 2 (S is off). Therefore, in general, for mode i ($i=1,2$), the state-space representation is presented in (1).

$$\begin{aligned} \dot{x} &= A_i x + B_i u \\ y &= C_i x \end{aligned} \tag{1}$$

where $x = \begin{bmatrix} i_1 & i_2 & v_1 & v_{dc} \end{bmatrix}^T$ are the defined system states, with superscript T denoting the transpose of the matrix. $A_1 = \begin{bmatrix} 0 & 0 & 0 & 0 \\ 0 & 0 & -\frac{1}{L_2} & -\frac{1}{L_2} \\ 0 & \frac{1}{C_o} & 0 & 0 \\ 0 & \frac{1}{C_{ultra}} & 0 & -\frac{1}{R_L C_{ultra}} \end{bmatrix}$, $B_1 = \begin{bmatrix} \frac{1}{L_1} & 0 & 0 & 0 \end{bmatrix}^T$ and $C_1 = \begin{bmatrix} 0 & 0 & 0 & 1 \end{bmatrix}$. Similarly, for mode 2, the defined state-space matrices are: $A_2 = \begin{bmatrix} 0 & 0 & -\frac{1}{L_1} & 0 \\ 0 & 0 & 0 & -\frac{1}{L_2} \\ \frac{1}{C_o} & 0 & 0 & 0 \\ 0 & \frac{1}{C_{ultra}} & 0 & -\frac{1}{R_L C_{ultra}} \end{bmatrix}$, $B_2 = B_1$ and $C_2 = C_1$. In general, the average large-signal model is obtained by combining the state equations where each state matrix of the averaged system is given by: $A = A_1 d + A_2 (1-d)$, $B = B_1 d + B_2 (1-d)$ and $C = C_1 d + C_2 (1-d)$, where d is the instantaneous duty ratio of the switch, S. In general, the large-signal dynamics of the Cuk converter can be presented as shown in (2), where d is the instantaneous value of the switch, S, duty ratio:

$$\dot{x} = A_2 x + B_2 + (A_1 - A_2)\, x d \tag{2}$$

Define: $x = x^{nom} + \Delta x$, where x^{nom} is the nominal (reference) value for the specific loading condition, and Δx is the perturbed value. Therefore, $i_1 = i_1^{nom} + \Delta i_1$, $i_2 = i_2^{nom} + \Delta i_2$, $v_1 = v_1^{nom} + \Delta v_1$, $V_{dc} = V_{dc}^{nom} + \Delta V_{dc}$, and $d = D^{nom} + \Delta d$. Using these definitions, the perturbed dynamics of the Cuk converter are presented in (3).

$$\begin{aligned} L_1 \tfrac{d\Delta i_1}{dt} &= -(1-d)\,\Delta v_1 + v_1^{nom} \Delta d \\ L_2 \tfrac{d\Delta i_2}{dt} &= -\Delta V_{dc} - (v_1^{nom} \Delta d + \Delta v_1 d) \\ C_o \tfrac{d\Delta v_1}{dt} &= \begin{bmatrix} \Delta i_1 - (i_1^{nom} \Delta d + \Delta i_1 d) \\ + (i_2^{nom} \Delta d + \Delta i_2 d) \end{bmatrix} \\ C_{ultra} \tfrac{d\Delta V_{dc}}{dt} &= \Delta i_2 - \tfrac{\Delta V_{dc}}{R_L} \end{aligned} \tag{3}$$

To design a control architecture based on the Lyapunov energy function, an energy function based on the state errors is defined and is presented in (4):

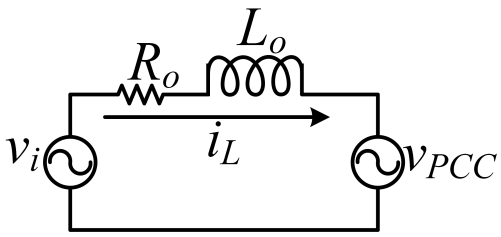

Fig. 3. Per-phase equivalent circuit of a three-phase inverter with RL filter

$$U = \frac{1}{2}L_1\Delta i_1^2 + \frac{1}{2}L_2\Delta i_2^2 + \frac{1}{2}C_1\Delta v_1^2 + \frac{1}{2}C_{ultra}\Delta v_{dc}^2 \quad (4)$$

Per the Lyapunov energy function-based controller architecture, the time derivative of (4) must be negative definite for some chosen user input to solve a tracking problem [11], [13], [14]. Therefore, using (3) and (4), the overall control law of the system is defined in (5):

$$d = D^{nom} + \Delta d = \\ -\frac{1}{v_1}\left(L_2\frac{di_2^{nom}}{dt} + V_{dc}^{nom}\right) - \gamma_o \begin{bmatrix} (v_1^{nom}\Delta i_1 - i_1^{nom}\Delta v_1) \\ -(v_1^{nom}\Delta i_2 - i_2^{nom}\Delta v_1) \end{bmatrix} \quad (5)$$

where γ_o is a user-defined constant chosen to accomplish the required bandwidth for the overall control architecture. In this work, four interleaved Cuk converters are considered, as shown in Fig. 1. Each one is operated independently based on (5) with interleaving to reduce the ripple on the inductor currents and capacitor voltages, thereby enhancing the effective switching frequency and reducing the component size. The next section outlines the AC-side control architecture, detailing the implementation of the advanced grid functionalities through the WEC.

III. Lyapunov Energy Function-Based Control of Inverter With Advanced Grid Support

In this section, we extend the Lyapunov energy function-based current control architecture introduced by [15]. A per-phase equivalent circuit diagram from the inverter poles to the PCC is presented in Fig. 3. This advanced control methodology leverages the modulation indices derived from the Lyapunov energy function, as extensively detailed in the prior research by [10], [13], [15]. This sophisticated approach is now applied within the $\alpha\beta$ coordinate system, enhancing its robustness and efficiency and accomplishing the reduction in the total number of equations involved considering a three-phase, three-wire system. The fundamental governing equations for the modulation indices, meticulously detailed in the referenced works, are pivotal for achieving precise current control in grid-connected inverters. These equations ensure the stability and performance of the control system by designing a control law based on the system's passive parameters as detailed in this section. To accomplish the overall control architecture, define: $x_\alpha = i_\alpha - i_\alpha^{ref}$ and $x_\beta = i_\beta - i_\beta^{ref}$. As elaborated in [15], to accomplish a Lyapunov energy function-based control architecture, the nominal (or the reference) dynamics as well as the measured or actual dynamics of the system are considered, and the corresponding error dynamics are presented in (6):

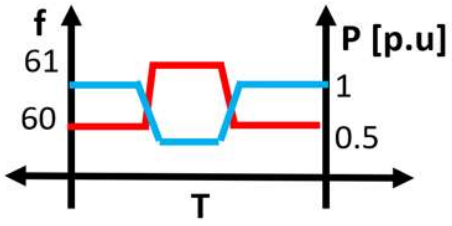

Fig. 4. $frequency - watt$ grid function

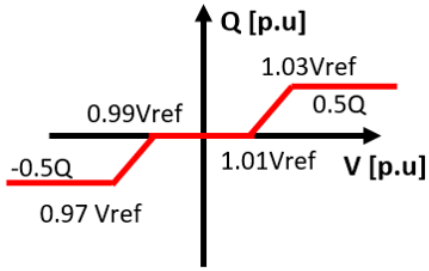

Fig. 5. $volt - VAr$ grid function

$$L_o\frac{dx_\alpha}{dt} = -x_\alpha R_o + \left(v_{i\alpha} - v_{i\alpha}^{ref}\right) \\ L_o\frac{dx_\beta}{dt} = -x_\beta R_o + \left(v_{i\beta} - v_{i\beta}^{ref}\right) \quad (6)$$

Let the modulation indices in the $\alpha\beta$ domain be defined as $m_\alpha = m_\alpha^{ref} + \Delta m_\alpha$ and $m_\beta = m_\beta^{ref} + \Delta m_\beta$, where the superscript ref quantities denote the reference, and Δ denotes the perturbed values. Consider now an energy function with an objective of solving a tracking problem as defined in (7):

$$\Omega = \frac{1}{2}L_o x_\alpha^2 + \frac{1}{2}L_o x_\beta^2 \quad (7)$$

To ensure negative definiteness of (7), the time derivative is carried out, and using (6), the overall expression is presented in (8):

$$\dot{\Omega} = x_\alpha \begin{pmatrix} v_{i\alpha} \\ -v_{i\alpha}^{ref} \end{pmatrix} + x_\beta \begin{pmatrix} v_{i\beta} \\ -v_{i\beta}^{ref} \end{pmatrix} - R_o \begin{pmatrix} x_\alpha^2 \\ +x_\beta^2 \end{pmatrix} \quad (8)$$

Finally, considering the sine pulse width modulation (PWM) and using these definitions, the overall control law for the AC-side three-phase inverter is presented in (9):

$$m_\alpha^{ref} + \Delta m_\alpha = \frac{2}{V_{dc}}\begin{pmatrix} L_o\frac{di_{L\alpha}^{ref}}{dt} + i_\alpha^{ref}R_o \\ +v_{PCC\alpha} - R_c x_\alpha \end{pmatrix} \\ m_\beta^{ref} + \Delta m_\beta = \frac{2}{V_{dc}}\begin{pmatrix} L_o\frac{di_{L\beta}^{ref}}{dt} + i_{L\beta}^{ref}R_o \\ +v_{PCC\beta} - R_c x_\beta \end{pmatrix} \quad (9)$$

where R_c is a user-defined constant chosen to achieve the required speed of convergence or bandwidth for the overall control architecture. To effectively manage and execute the grid functionalities, a comprehensive hierarchical control framework has been established integrating two major advanced grid support functions: $frequency{-}watt$ and volt-volt ampere reactive ($volt - VAr$). These strategies are qualitatively illustrated in Figs. 4 and 5, respectively, demonstrating their critical roles in maintaining grid stability and performance. The reference signals for the currents generated for the Lyapunov energy function-based controllers are modified based on the grid conditions (voltage/frequency) to incorporate these advanced grid functions based on IEEE-1547 [12]. By leveraging these control strategies, the system can dynamically

TABLE I
PLANT AND COMPENSATOR PARAMETERS

Parameter	Value
Power rating (each $DC-DC$)	1 kVA
Power rating (two-level inverter)	5 kVA
v_o	650 V
v_{dc}	900 V
v_{PCC}	208 V
L_1	0.5 mH
L_2	0.5 mH
C_o	80 μF
C_{ultra}	1 F
R_o	0.5 Ω
L_o	4.2 mH
f_{dc-dc}	20 kHz
$f_{inverter}$	20 kHz
γ_o	80
R_o	70

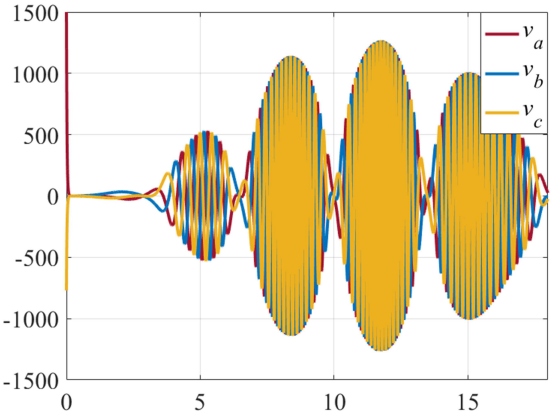

Fig. 6. Three-phase voltage generated from the wave energy generator

respond to voltage and frequency fluctuations, optimize power quality, and enhance grid resilience. The detailed integration of these control mechanisms within the local control architecture underscores the robustness and efficiency of the proposed control framework, thereby ensuring the reliable and efficient operation of the grid-connected system. This comprehensive control methodology not only facilitates seamless operation under normal conditions but also provides robust performance during grid disturbances, contributing to the stability and reliability of modern power systems. To verify the effectiveness of the proposed system, the subsequent section provides a detailed implementation of the proposed strategy within the $MATLAB/Simulink$ environment. This section meticulously outlines the simulation setup and parameters, showcasing how the strategy is applied in a controlled, virtual setting. Additionally, the section highlights several key case studies, illustrating the system's performance under various scenarios. These case studies are selected to demonstrate the robustness, efficiency, and adaptability of the proposed control framework, providing comprehensive insights into its practical applicability and potential benefits for grid-connected systems.

IV. RESULTS AND DISCUSSIONS

The overall system is modeled in MATLAB/Simulink, and various case studies are presented. The simulation parameters are collectively presented in Table I (NOTE: The x-axis in the

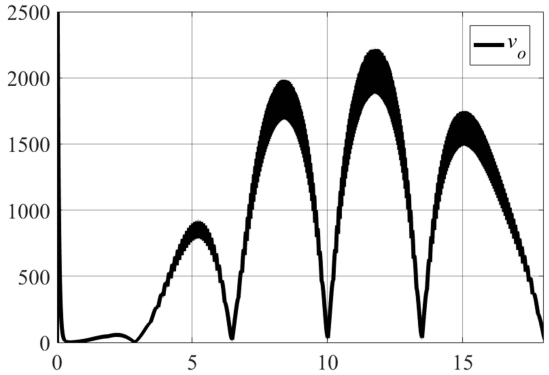

Fig. 7. DC voltage after the diode rectifier

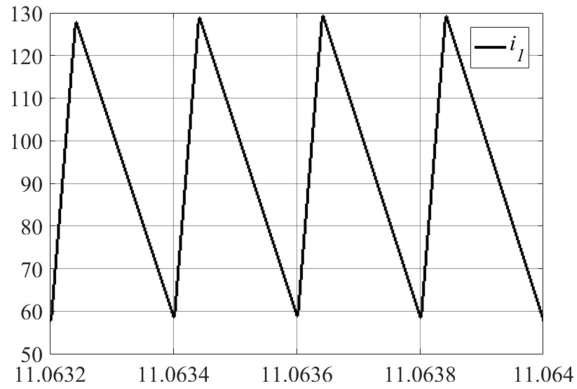

Fig. 8. Inductor current on the input side of a single Cuk converter

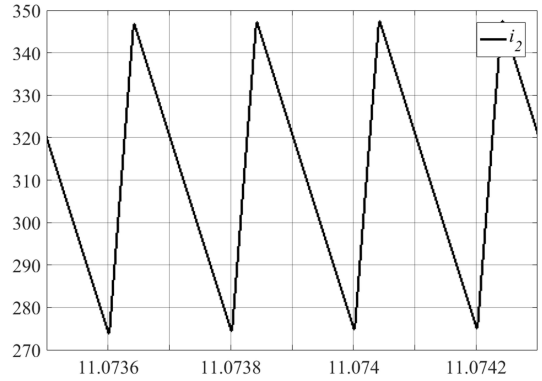

Fig. 9. Inductor current on the output side of a single Cuk converter

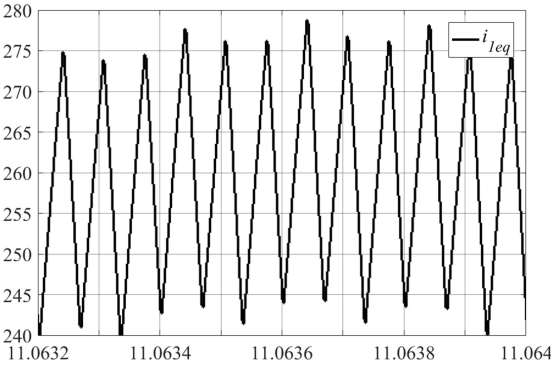

Fig. 10. Equivalent inductor current on the input side of a Cuk converter

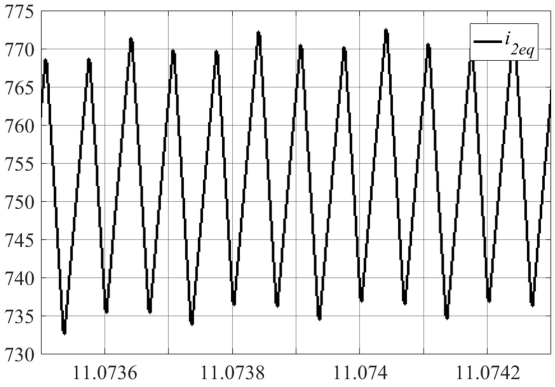

Fig. 11. Equivalent inductor current on the output side of a Cuk converter system

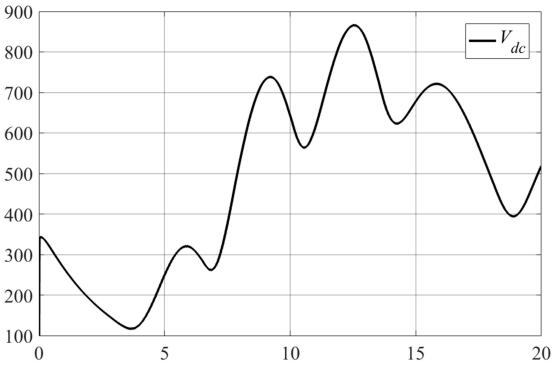

Fig. 12. DC bus voltage of the input to the two-level inverter with four interleaved Cuk converters

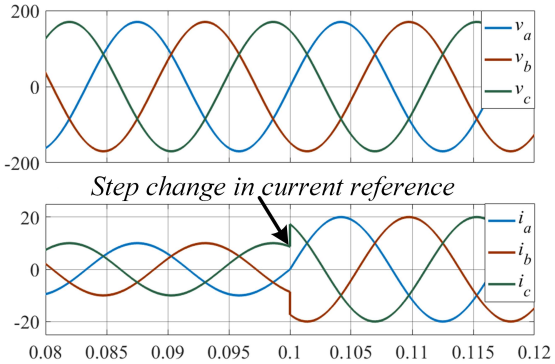

Fig. 13. Step change in line current on the AC side

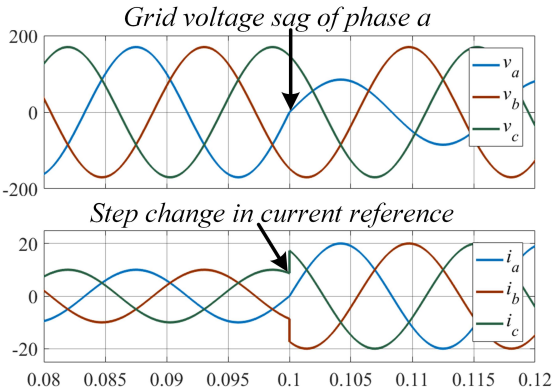

Fig. 14. Step change in line current on the AC side during a grid voltage sag on phase a at the same instant

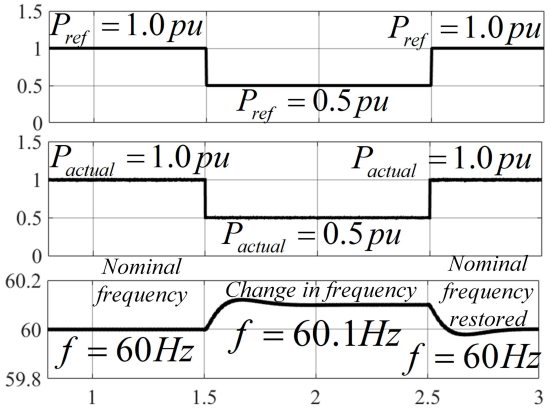

Fig. 15. Change in active power on the grid side during a symmetrical change in frequency (in pu)

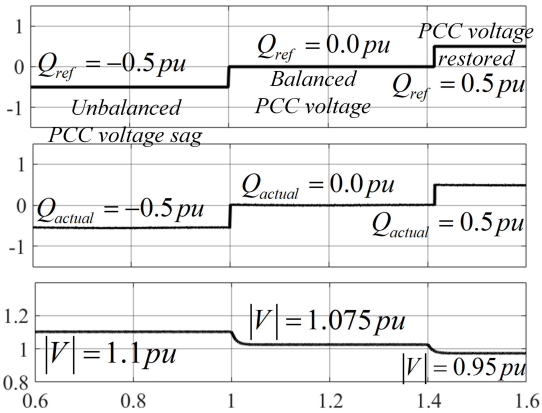

Fig. 16. Change in reactive power on the grid side during a symmetrical change in voltage magnitude (in pu)

results represents time in seconds, while the y-axis indicates either volts or amps for voltage and current measurements, and per-unit values for active and reactive powers.). Several important case studies are being considered to understand the effectiveness of the proposed approach. The results showing the three-phase voltages generated by the wave generator and its equivalent DC voltage, v_o, obtained from the diode rectifier are presented in Figs. 6 and 7, respectively. These show the fluctuating nature of the wave energy-generated power and the need for the ultra-capacitors downstream. Next, the results showing the performance of the Lyapunov energy function-based controller for a single Cuk $DC-DC$ converter are presented. The results showing the currents i_1 and i_2 for the inductors L_1 and L_2 of Fig. 2 are presented in Figs. 8 and 9 (zoomed), respectively. These results show the input and the output current of the Cuk converter with the implemented control architecture. The results showing the equivalent input and output current of the Cuk-based $DC-DC$ converter system are presented in Figs. 10 and 11 (zoomed), respectively. These results indicate the significant reduction in the overall ripple content showing the overall increase in the equivalent switching frequency with proper interleaving. This property enables the reduction in the size of the passive components, thereby reducing the size and the overall cost of implementation of the system. A similar result for the DC bus voltage with four interleaved Cuk-based $DC-DC$ converters

is presented in Fig. 12. In this case, only the output DC voltage is of interest, which serves as the input to the three-phase, two-level inverter that interconnects this whole system to the grid. Note that although the switching ripple on the DC voltage is negligible, for the physical nature of the wave energy availability, wide fluctuations are observed on the c_{ultra} voltage. Nevertheless, a seamless PCC current (power) can still be maintained with the proposed WEC system. Next, the focus is to check the overall controller performance for the AC-side inverter system interconnecting the wave generator to the PCC with the wide fluctuations in the available wave power. The results showing the PCC voltage during a step change in the line current reference is shown in in Figs. 13. These results indicate the seamless performance of the AC-side Lyapunov energy function-based controller with superior dynamic performance. The next results show the worst type of dynamics for the AC side, where the step change in the line current reference and an unbalanced grid voltage sag for phase a occurs at the same instant of time, as presented in Figs. 14. These results show the advanced disturbance rejection capability for the AC-side controller. Finally, the results showing the advanced grid support functions for the overall system are presented. The results shown in Fig. 15 present the implementation of the $frequency - watt$ grid functionality. Similarly, the results in Fig. 16 show the successful implementation of the $volt - VAr$ grid functionality. These results indicate the potential for advanced grid support functionalities with the WEC and the implemented advanced control architecture. The system shows promise in contributing to grid stability and resilience, effectively managing frequency and voltage fluctuations. The control architecture's superior dynamic performance and disturbance rejection enhance the $WEC's$ role in grid management. This will include extensive simulations and experimental validations to confirm the system's efficacy and practical applicability, providing valuable insights into its capabilities and contribution to sustainable energy solutions.

V. Conclusion

This paper introduces a cutting-edge approach to wave energy collection through an interleaved Cuk converter system. The wave energy converter is connected to a three-phase diode rectifier, which feeds input to four interleaved Cuk $DC - DC$ converters. The system's states, controlled by an architecture based on the Lyapunov energy function, exhibit exceptional dynamic performance and disturbance rejection capabilities. The results demonstrate consistent and reliable dynamic behavior for the AC-side states under both normal and abnormal grid voltage conditions, underscoring the superior effectiveness of the proposed control strategy. Moreover, the implementation of advanced grid support functions enables the system to prevent outages during frequency or voltage deviations, significantly enhancing grid stability. The robustness and efficiency of the proposed system position it as a promising candidate for improving grid reliability in renewable energy applications. Extensive simulations and experimental validations further confirm the system's reliability and practical viability, making it well-suited for real-world deployment. Future research will focus on optimizing the system for even greater efficiency and exploring deployment in various real-world scenarios to facilitate broader adoption. The insights and advancements presented in this study contribute to the development of more resilient and efficient renewable energy systems, offering a substantial step forward in sustainable energy solutions. Additionally, the system's ability to maintain performance under challenging conditions highlights its potential to support the growing demand for reliable and clean energy sources.

References

[1] X. Zhou, S. Zou, W. W. Weaver, and O. Abdelkhalik, "Assessment of electrical power generation of wave energy converters with wave-to-wire modeling," *IEEE Transactions on Sustainable Energy*, vol. 13, no. 3, pp. 1654–1665, 2022.

[2] B. A. Ling, B. Bosma, and T. K. A. Brekken, "Experimental validation of model predictive control applied to the azura wave energy converter," *IEEE Transactions on Sustainable Energy*, vol. 11, no. 4, pp. 2284–2293, 2020.

[3] G. Bacelli and J. V. Ringwood, "Numerical optimal control of wave energy converters," *IEEE Transactions on Sustainable Energy*, vol. 6, no. 2, pp. 294–302, 2015.

[4] O. Farrok, M. R. Islam, M. R. Islam Sheikh, Y. Guo, J. Zhu, and G. Lei, "Oceanic wave energy conversion by a novel permanent magnet linear generator capable of preventing demagnetization," *IEEE Transactions on Industry Applications*, vol. 54, no. 6, pp. 6005–6014, 2018.

[5] J. S. Park, B.-G. Gu, J. R. Kim, I. H. Cho, I. Jeong, and J. Lee, "Active phase control for maximum power point tracking of a linear wave generator," *IEEE Transactions on Power Electronics*, vol. 32, no. 10, pp. 7651–7662, 2017.

[6] J. A. Leon-Quiroga, G. Bacelli, D. D. Forbush, S. J. Spencer, and R. G. Coe, "An efficient and effective wec power take-off system," *IEEE Transactions on Sustainable Energy*, vol. 14, no. 3, pp. 1526–1539, 2023.

[7] E. Tedeschi, M. Carraro, M. Molinas, and P. Mattavelli, "Effect of control strategies and power take-off efficiency on the power capture from sea waves," *IEEE Transactions on Energy Conversion*, vol. 26, no. 4, pp. 1088–1098, 2011.

[8] E. A. Amon, A. A. Schacher, and T. K. A. Brekken, "A novel maximum power point tracking algorithm for ocean wave energy devices," in *2009 IEEE Energy Conversion Congress and Exposition*, 2009, pp. 2635–2641.

[9] H. Komurcugil., "Passivity-based control of single-phase PWM current source inverters," in *Proc. IEEE Industrial Electronics Society Conf. (IECON).*, 2007, pp. 545–550.

[10] H. Komurcugil, "Improved passivity-based control method and its robustness analysis for single-phase uninterruptible power supply inverters," *IET Power Electronics*, vol. 8, pp. 1558–1570, Mar 2015.

[11] K. Hasan, "Passivity-based control of single-phase pwm current-source inverters," in *IECON 2007 - 33rd Annual Conference of the IEEE Industrial Electronics Society*, Taipei, Taiwan, November 2007.

[12] IEEE Standards Association, "IEEE standard for interconnection and interoperability of distributed energy resources with associated electric power systems interfaces," in *IEEE Std 1547-2018 (Revision of IEEE Std 1547-2003) - Redline*, 2018, p. 1–227.

[13] H. Komurcugil, N. Altin, S. Ozdemir, and I. Sefa, "Lyapunov-function and proportional-resonant-based control strategy for single-phase grid-connected VSI with LCL filter," *IEEE Transactions on Industrial Electronics*, vol. 63, pp. 2838–2849, May 2016.

[14] I. Sefa, S. Ozdemir, H. Komurcugil, and N. Altin, "An enhanced lyapunov-function based control scheme for three-phase grid-tied vsi with lcl filter," *IEEE Transactions on Sustainable Energy*, vol. 10, pp. 504–513, April 2019.

[15] V. R. Chowdhury, "Internal model based grid voltage estimation and control of a three-phase grid connected inverter for *pv* application," *IEEE Transactions on Energy Conversion*, vol. 36, no. 4, pp. 3568–3577, 2021.